Method Article

Clay minerals identification in rock varnish by XRD: A one-step reduction approach

Amritpal Singh Chaddha [a,b], Anupam Sharma [a,*], Narendra Kumar Singh [b]

[a] Birbal Sahni Institute of Palaeosciences, Lucknow-226007, India
[b] Department of Chemistry, University of Lucknow, Lucknow-226007, India

a b s t r a c t

Rock varnishes are known to be fine, dark, glossy submicron films found in deserts bare rock surfaces. The oxides and hydroxides of manganese and iron bind bind together the clay minerals present in the varnish layer. The processes of oxide-hydroxide accumulation at varnish sites are due to iron and manganese oxidizing bacteria which may require clay minerals for additional nutrition. Quantification and identification of clay minerals in this biofilm is needed to understand its formation. Past attempts to analyze the mineralogical composition of rock varnish have led to inconclusive results as varnish is a submicron thin layer composed of a complex mineral matrix. The elimination of non-crystalline cementing groups comprising of free iron oxides is a key step in the identification of many types of clay minerals, particularly in soil/sediment mineral studies.

- The Fe-Mn oxide-hydroxide coatings, acting as cementing materials, can be easily removed using a one-step reduction method employing $Na_2S_2O_4$ at 70 °C, leading to separation of clay minerals.
- We have taken the lead from earlier reported Jackson (1958) method, wherein a combination of reagents was used such as sodium acetate, sodium citrate, hydrogen peroxide, sodium bicarbonate, and sodium dithionite for removing carbonate, organic carbon and Fe-Mn oxy-hydroxide coatings respectively from sediment grains to segregate individual grains from each other.
- Our modification helps in the unveiling of clay minerals from a solid substrate and reports the X-ray diffraction peaks, which are elsewise hard to detect and therefore earlier studies are inconclusive.

* Corresponding author.
  E-mail address: Anupam110367@gmail.com (A. Sharma).

Specifications table

Subject Area	Earth and Planetary Sciences
More specific subject area	Mineralogy, Geochemistry, Palaeoclimate
Method name	Iron-Manganese Oxide-Hydroxide Removal from Soils and Clays by a Dithionite-Citrate System Buffered with Sodium Bicarbonate
Name and reference of original method	Mehra, O.P., Jackson, M.L. Iron Oxide Removal from Soils and Clays by a Dithionite-Citrate System Buffered with Sodium Bicarbonate. Clays Clay Miner. 7, 317–327 (1958). 10.1346/CCMN.1958.0070122
Resource availability	N.A

Method details

Background

X-ray diffraction is an analytical technique widely used for crystalline phase identification including minerals [1]. However, naturally occurring non-crystallized materials such as amorphous phases and biomarkers sometimes mask the crystalline phases making the work challenging, as observed in various research operations across the globe. One such example is dropping the Mars-XRD instrument from the ExoMars rover, in 2012 [2], to curtail the payload of the ExoMars Mission. Therefore, mineralogical analysis of varnish surfaces, or similar material existing on Mars rocks has always been a challenge, even for such escalated missions. Identification of mineral pattern on varnish is not straightforward, because it is a complex mixture mainly composed of iron and manganese oxides cemented with various clay minerals [3].

One more problem associated with iron and manganese elements is X-ray fluorescence phenomenon, which is an undesirable phenomenon in XRD, resulting in loss of a relatively large part of the energy of the incident beam in the due process. This leads to lowering of the intensity of the diffracted beam resulting in a high back- ground, making certain peaks undetectable, and hence difficult to analyze on the diffractogram [4].

To develop a better understanding of rock varnish, the study of clay minerals cannot be ignored. However, the separation of clay from sediments and soils, is an extensive and tedious process [5]. It is also reported that the importance of clays in varnish formation has a vital impact on oxides formation in the varnish layer [6]. Hence, it is necessary to remove amorphous coatings and crystals of free iron and manganese oxides from varnish deposited on rock substrates because iron and manganese cause fluorescence of X-Ray diffractograms, obscuring the clay peaks [7].

Detailed methodology

Rock varnish sample were collected (Fig. 1a) from Ladakh batholith boulder ($\sim$85–45 Ma) [8–10]and subjected to microscopic studies (Fig. 1b) to observe the surface thickness and morphology of the varnish layer. Petrographic studies of thin sections of the rock varnish sample were conducted to identify minerals of the rock varnish sample (Fig. 1c, d). However, mineral composition in the varnish layer was not providing a complete array as observed in the host rock displaying the following: Quartz, Plagioclase, Feldspar, Biotite, and Hornblende) (Fig. 1c, d).

FESEM-EDS analysis (Field Emission Scanning Electron Microscopy-Energy Dispersive X-Ray Spectroscopy) was conducted on a thin section of rock varnish to see the morphological features of layer and host rock along with its elemental composition (Fig. 1e, f).

Further, a chip of rock varnish sample was subjected to electron microscopic analysis for detailed investigation of varnish layer and its host rock morphology (Fig. 2a) alongside chemical characterization with multi-spot energy dispersive X-ray microanalysis (Fig. 2b, c).The weight percentage ratios of Si/Al calculated from multi-spot EDS analysis in the varnish layer corresponds to 1.34 with higher *K* content, substantiating presence of Illite in the layer. Moreover higher Mn and Fe content in the varnish layer also suggest the presence of chlorite in the layer. Contrary to it, Si/Al ratio in the host rock is $\sim$3.0, which confirms plagioclase phase [11,12]. Therefore, it is certain that
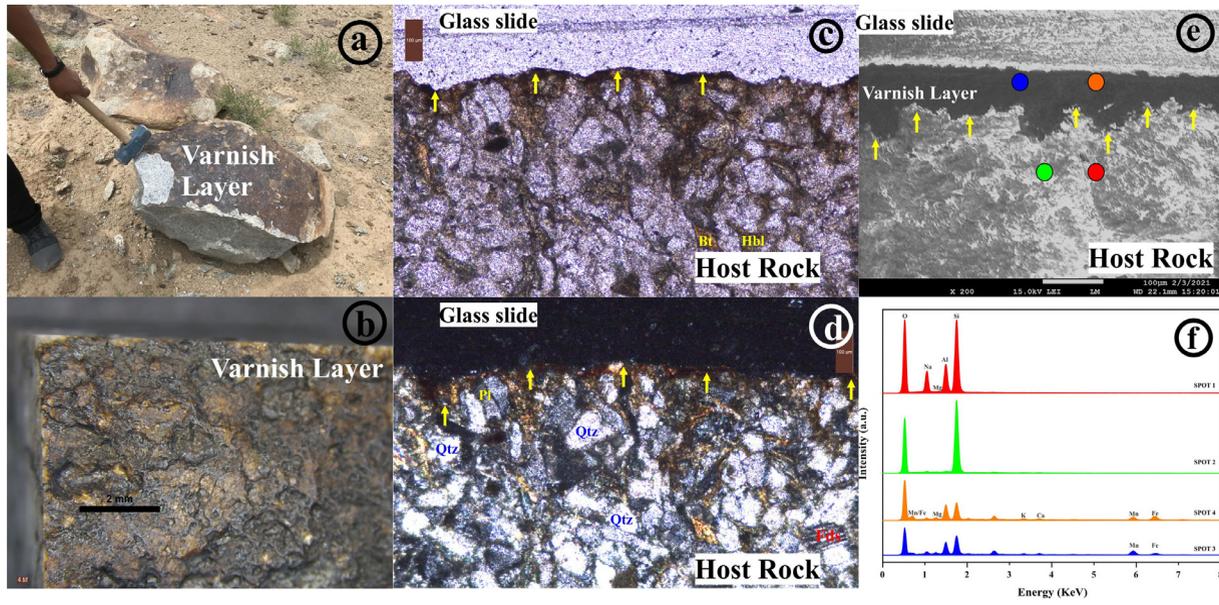
Fig. 1. (a) Rock Varnish sample in the field; (b) Optical microscopic image of varnish Layer; (c) Thin section slide of a cross-section of varnish sample in plane-polarized Light at 10x; (d) Thin section slide of a cross-section of varnish sample in crossed polarized Light at 10x; (e) FE-SEM (Scanning electron microscopy) image of a thin section of the Rock varnish sample at 200x depicting contrast morphology between layer and host rock; (f) Multi-spot EDS analysis of rock varnish thin section showing different elements present in the varnish layer viz. Si, Al, Mg, K, Ca, O with (Mn, Fe) enrichment and host rock showing (Na, Al, Si, Mg, O, K).
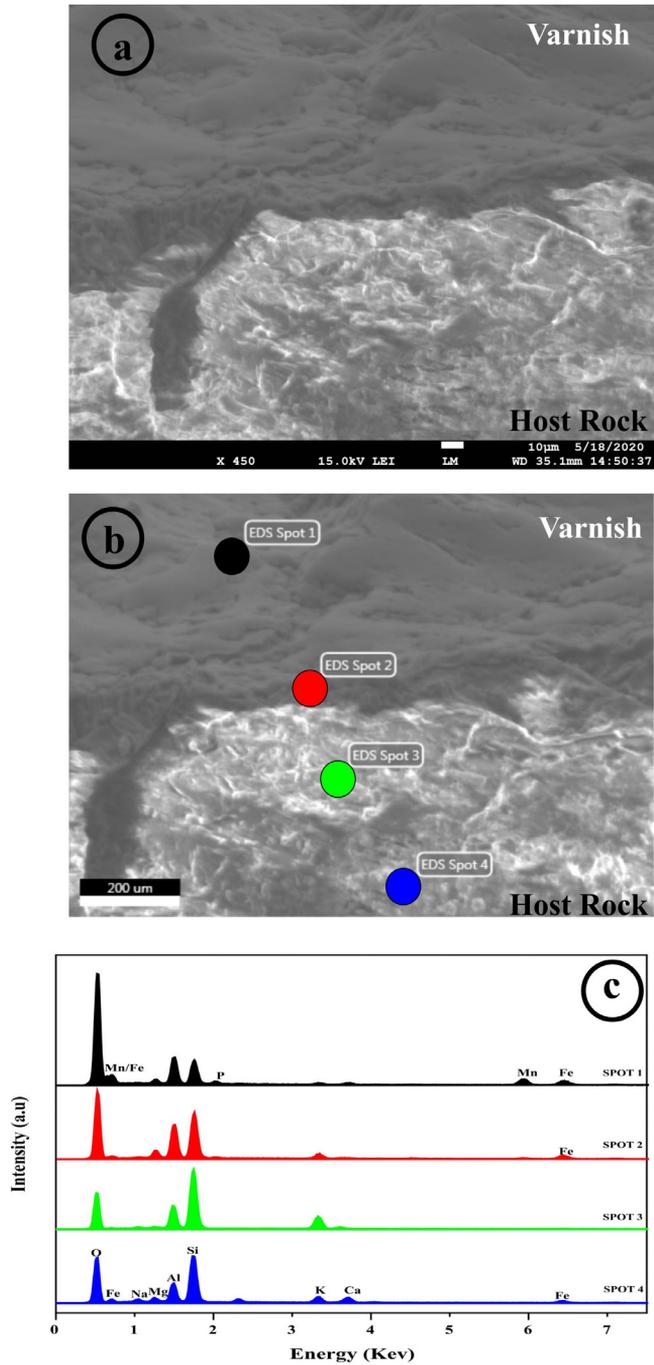
Fig. 2. (a) Detailed examination of the Rock varnish sample using FE-SEM imaging at 450x revealed layered morphology of varnish layer affixed on host rock with boundary delimitation between varnish layer and host rock; (b, c) Multi-spot elemental analysis of rock varnish layer and host rock exhibit different elemental presence in the varnish layer and host rock.

there is no altered film formed during the scrapping process, confirming no cross contamination from the drilling bit used.

Identification of clay minerals in the petrographic analysis has been difficult to study in the past due to their very fine sheet structure and subtle variation in chemical composition between these minerals and among other silicates [13], therefore, to further confirm the minerals of the varnish layer separated from the rock substrate, it was subjected to X-ray diffraction studies. A specific methodology proposed by Jackson [14] was applied to study the complex mineralogical matrix of the varnish sample. Our one-step reduction methodology, slightly different from the Jackson method, where a combination of chemical reagents was used, is depicted in Fig. 3.

The steps followed are given below:

1 The rock varnish sample was extracted carefully using Dremel Micro drill (Model no. 800 Dremel) with diamond coated coarse bit to avoid contamination while scrapping out the varnish layer from the underlying host rock [15] and stored in a small Eppendorf tube.

2 The drilled sample was subjected to Powder XRD on a silicon substrate zero background holder on an X-Ray Diffractometer (PANalytical Xpert'3 Powder) and was irradiated with (Cu Kα1 = 1.540598 Å; Kα2 = 1.544426 Å).

3 The diffraction pattern was reported from 5 ° to 70 ° of 2θ range (step size (°2θ) = 0.0130, scan time = 32 s per step), at room temperature.

4 As a result, the corresponding XRD diffractogram of the varnish layer of rock surface was formulated (Fig. 5a).

5 Subsequently, 0.2 g of the drilled sample was transferred to a clean and dry beaker.

6 Next, the beaker was placed on a magnetic stirrer with a hot plate with a temperature set to 70 °C.

7 Once the temperature is attained, 1% $Na_2S_2O_4$ solution was transferred dropwise to the beaker containing the powdered sample, and the reaction was set up for 1 h at 70 °C.

8 After 1 h, the reaction mixture was centrifuged at 2500 rpm for 6 min. Following this, the filtrate was discarded and the obtained residue was washed with deionized water 3 times with constant shaking.

9 After washing the sample, it was subjected to centrifugation again.

10 Finally, the residue was dried in the oven at 40 °C. This dried and treated sample was then analyzed on an X-ray diffractometer and its diffractogram was obtained (Fig. 5b)

11 To confirm the clay mineral signatures obtained under treated sample diffractogram (Fig. 5b), steps 5 to 9 were repeated with a requisite amount of drilled sample to prepare oriented clay slides, as emphasized by Moore & Reynolds (1997).

12 The clay fractions prepared by centrifugation technique were transferred to a glass substrate.

13 Air-dried, heated and ethylene-glycol solvated slides were prepared and positioned on a XRD stage. (Fig. 4a, b)

14 Eventually, these oriented samples were positioned on XRD stage and run on the diffractometer (air-dried) and then analyzed again following various treatments such as solvation with ethylene glycol, and heating to a specified temperature of 550 °C for 1 h. (Fig. 4a, b)

15 The diffraction pattern for each clay slide (air-dried, heated, glycolated) was recorded with step size (°2θ) = 0.0130, scan time = 48 s per step (Fig. 6 a–c) and presence of clay minerals was confirmed respectively.

Method validation

The formulated method was validated and found to be successful as we compared the X-Ray diffractograms of the pre-treated rock varnish sample with the reduced rock varnish sample (Fig. 5a, b). The contrasting behavior was evident that the X-ray peaks corresponding to the clay minerals present in the rock varnish layer were now distinguishably visible (Fig. 5b), which were otherwise incognito/not clear (Fig. 5a). Additionally, the pre-treated varnish sample show peaks corresponding to Quartz, Plagioclase, and Manganese hydroxide matched with (ICDD/ PDF-4 database file No. 01-075-8320, 00-003-0499, 04-005-8804) respectively on PANalytical High Score Software.

MODIFIED APPROACH

Rock Varnish Sample + 1 g
$Na_2S_2O_4$

70°C, Magnetic
stirrer with hot
plate, 1 hour

Centrifugation + washing
with Distilled Water

Leaching of iron oxides via
reducing Fe (III) ⟶ Fe (II)

OLD APPROACH

Sample + Na-acetate solution in centrifuge tube

80°C, water bath, 1 hour

Cooling followed by three time centrifugation

Add H_2O_2 dropwise

80°C, water bath, 1 hour/
Centrifugation &

1 M $NaHCO_3$ solution + Na – citrate solution

Water bath, 20 min

1 g $Na_2S_2O_4$

Water bath, 1 hour

Cooling and Centrifugation

Leaching out of iron and manganese oxides

Modification

Fig. 3. The methodology proposed by He [7] is primarily used in removing the coatings of carbonates, organics, and Fe-Mn oxide-hydroxide in soil and sediments, which resulted in aggregates and coagulation of grains, however, the rock varnish is mainly Fe-Mn rich layer and therefore, the proposed one-step method is sufficient to serve the purpose.
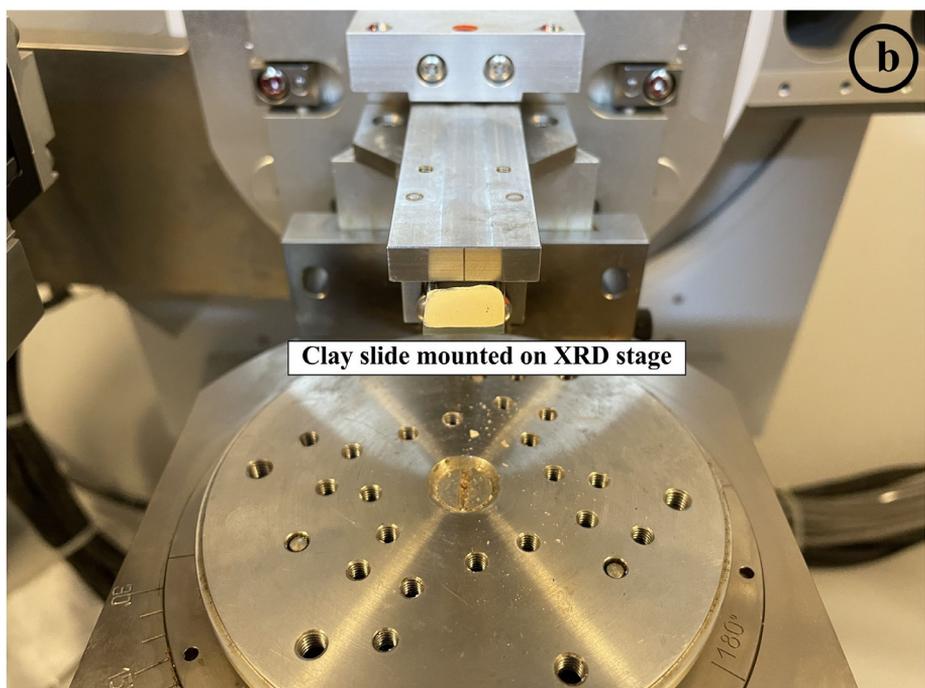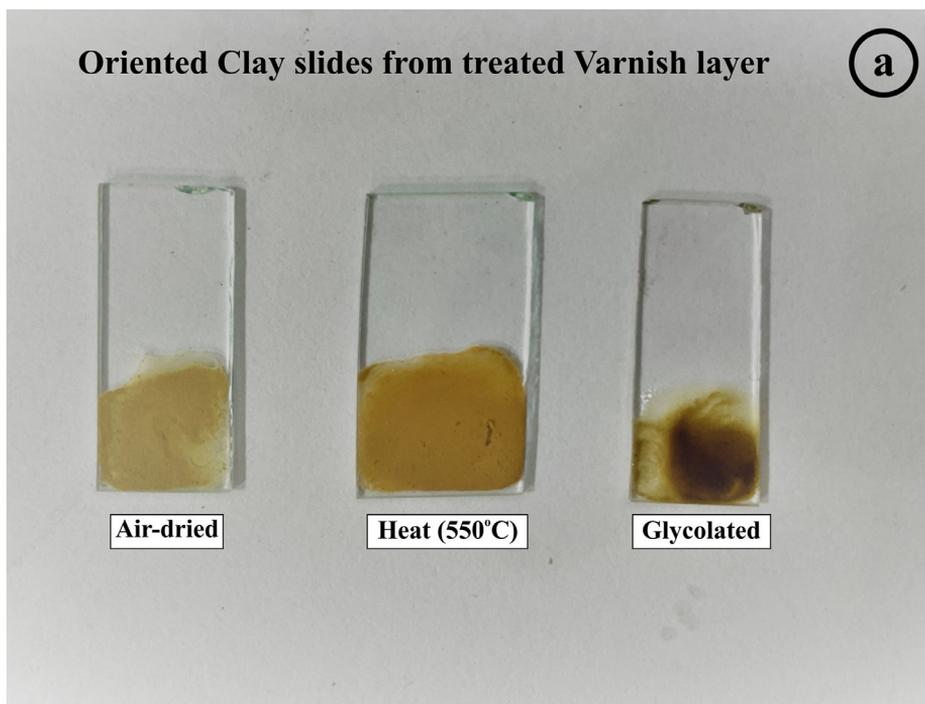
Fig. 4. (a) Preparation of oriented clay slides on glass substrate from reduced varnish layer with air dried, heated (at 550 °C), glycolated fractions respectively; (b) Mounting of prepared clay slides onto the multipurpose flat XRD stage.
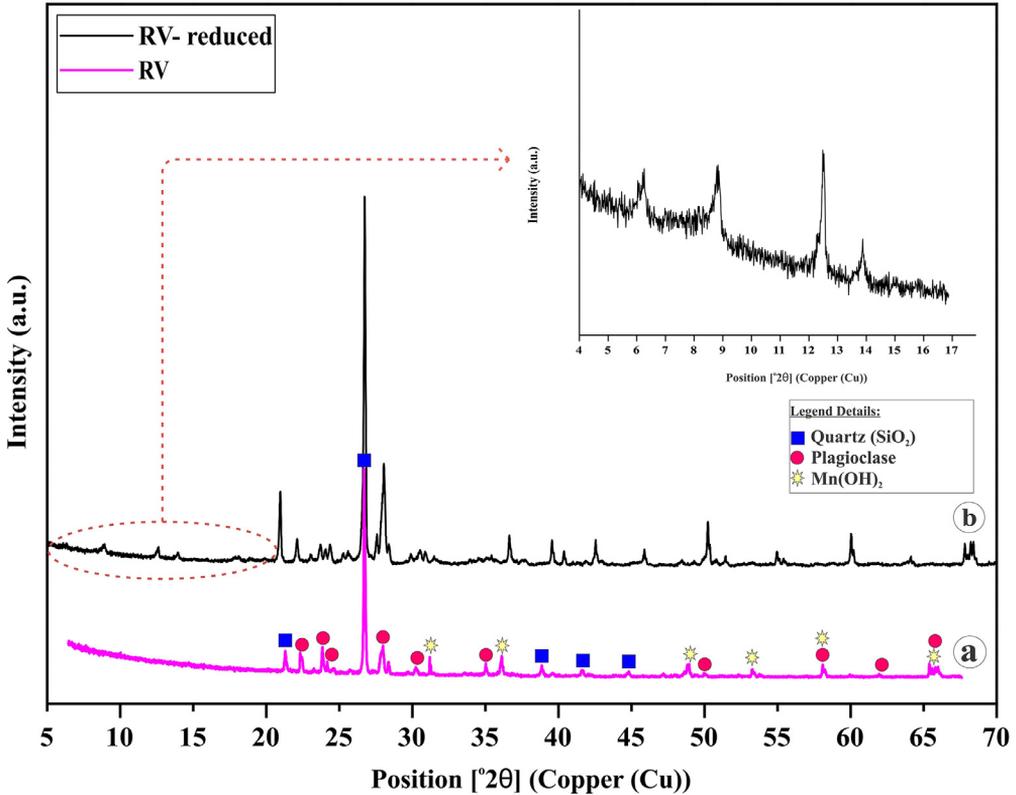
Fig. 5. (a) XRD diffractogram showing the mineralogy of varnish layer present on the host rock; (b) XRD diffractogram of reduced varnish layer depicting the presence of various clay minerals, which is otherwise unclear because of the complex mineralogical moiety of the varnish layer.

In order to confirm the clay minerals signatures obtained from treated varnish sample (Fig. 5b), which was XRD pattern from an air-dried random specimen, it is always better to validate the results by preparation of oriented clay slides [16,17].

Therefore, air-dried, heated and glycolated clay slides (Fig. 6a–c) displayed Chlorite, Illite as the main components of clay minerals in the rock varnish sample (Table 1) present in the complex moiety of the rock varnish layer along with the other non-clay minerals as deduced in (Fig. 5b).

To substantiate the difference between chlorite and kaolinite minerals, heat treatment was performed resulting in retention of 7.0 Å diffraction peak and increase in intensity of 14.1 Å (001) peak in chlorite. Additional basal reflection $d = (001)$ is constant for Illite = 10 Å, and is recognized on X-ray diffractogram by its strong first-order basal (001) peak at ∼10 Å and successive second order (002) peak, follows an integral order of reflection showing peak at ∼5.0 Å [18]. A supportive verification of illite can be deduced from the glycolated fraction which shows almost no expansion on ethylene glycol solvation and no shift is observed [19].

Additionally, crystallinity index (IC) of basal peak for Illite generally expressed in $°\Delta 2\theta(\Delta 2\theta=$XRD angle) was calculated by measuring the Full width half maxima (FWHM) of ∼10 Å peak [20], and was found to be 0.35 $°\Delta 2\theta$. It is suggestive of anchizonal metamorphism signatures that results from discrete mineral reactions visible specifically in clay minerals thereby confirming the presence of Illite fractions [21–23].

Further, phase identification and peak indexing of chlorite and Illite in the varnish layer were obtained by matching the crystallographic information file from COD ID: 9000132 and 9013718 using crystallography open database [24,25].
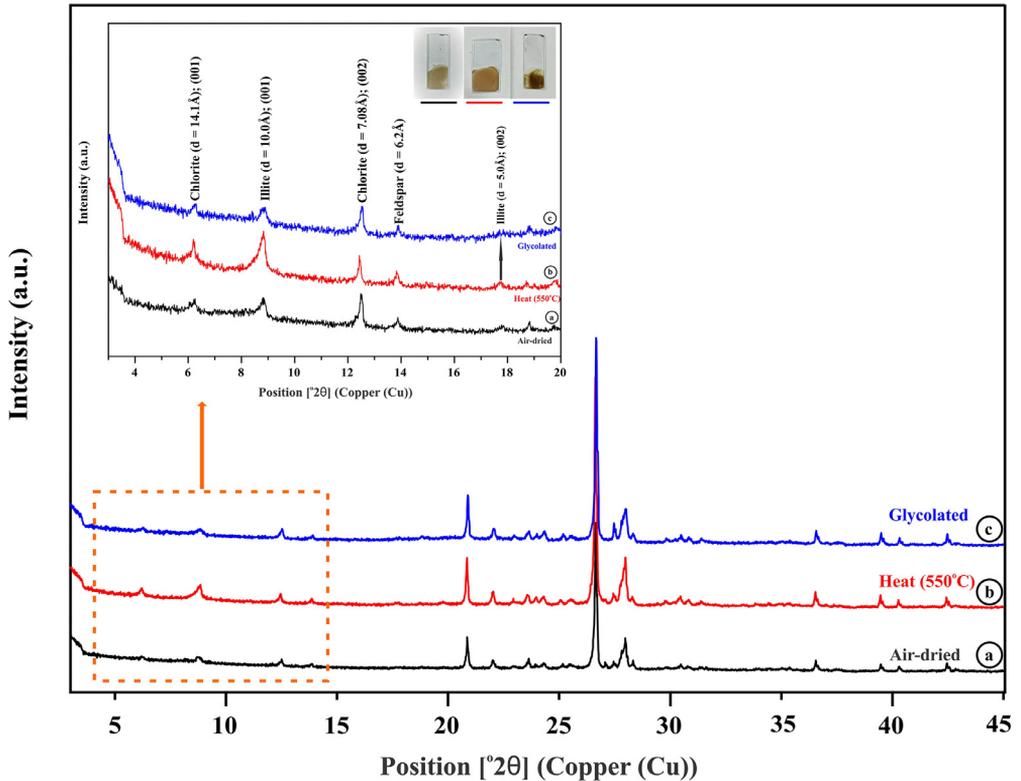
Fig. 6. Complete XRD patterns for (a) air-dried; (b) heated (at 550 °C); (c) EG-solvation clay fractions of treated varnish layer sample with inset image clearly showing the diffraction peaks at lower angles.

Table 1
XRD diffraction peaks for the clay minerals present in Reduced varnish sample slides [28].

S. No.	REDUCED VARNISH SAMPLE		
	Mineral	d-spacing (Å)	Degree (2Θ)
1	Chlorite (001)	14.1	6.1
2	Illite (001)	10.0	8.7
3	Chlorite (002)	7.08	12.4
4	Illite (002)	5.0	17.7

Rietveld analysis [26] of the complete experimental XRD pattern was done on the powdered varnish layer sample (Fig. 7a) using High score software [27] and the pattern was matched with standard known CIF files from ICDD and ICSD databases viz. 00-022–0675(Microcline-Feldspar), 01-087–2096(Quartz), 98–008–7657(Albite), 98–020–1648(Anorthite), 98–015–2289(Birnissite), 98–018–7569(Muscovite) phases with respective percentages of the mineral phases present in the sample as shown in (Fig. 7a).The differences were minimized with the application of a refinement procedure which can been seen in form of difference plot between experimental and calculated pattern (Fig. 7b) The results obtained showed a good fit with agreement indices values viz. $\chi^2 = 1.6$; R_p (%) = 7.8; R_{wp}(%) = 10.8; R_{exp}(%) = 6.5. Detailed information about the CIF files and parameters used for refinement is given in the supplementary file (Rietveld supplementary).

Therefore, it can be concluded that the successful reduction of varnish layer with $Na_2S_2O_4$ resulted in leaching out of amorphous Fe/Mn oxides thereby paving way for recording a clear XRD
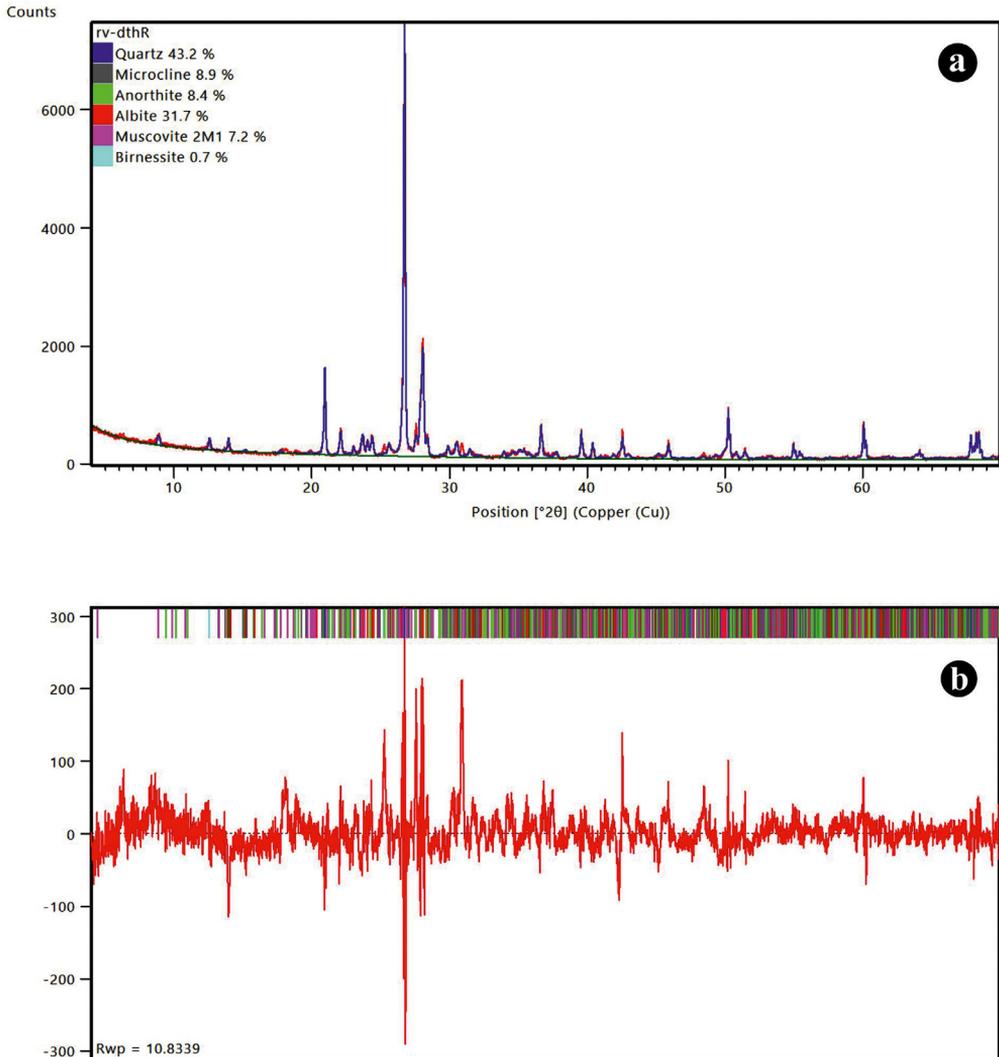
Fig. 7. (a) Rietveld refined Powder XRD pattern showing the mineral phases present in the rock varnish sample; (b) Difference plot between experimental and calculated XRD pattern for Rietveld refinement.

Diffractogram of the clay minerals (Fig. 6) and provides a better understanding of the minerals, otherwise subdued due to complex mineralogical moiety in rock varnishes.

Declaration of Competing Interest

The authors declare that they have no known competing financial interests or personal relationships that could have appeared to influence the work reported in this paper.

Acknowledgments

Facility for providing access to analytical facilities needed in the study and Dr. S.K. Pandey and Mr. Harsh for helping out in carrying the petrography study. Special thanks to Dr Mangesh for providing additional technical support in the analysis. We also thank the anonymous reviewer(s) for their many insightful comments and suggestions which has helped in improving the manuscript.

Supplementary materials

Supplementary material associated with this article can be found, in the online version, at doi: 10.1016/j.mex.2021.101511.

References

[1] C. Malherbe, I.b. Hutchinson, R. Ingley, A. Boom, A.s. Carr, H. Edwards, B. Vertruyen, B. Gilbert, G. Eppe, On the habitability of desert varnish: a combined study by micro-Raman spectroscopy, X-ray diffraction, and methylated pyrolysis–gas chromatography–mass spectrometry, Astrobiology 17 (2017) 1123–1137, doi:10.1089/ast.2016.1512.

[2] L. Marinangeli, I. Hutchinson, A. Baliva, A. Stevoli, R. Ambrosi, F. Critani, R. Delhez, L. Scandelli, A. Holland, N. Nelms, Mars-Xrd Team, An European XRD/XRF instrument for the ExoMars mission, 38 (2007) 1322.

[3] E.P. Vicenzi, C.A. Grissom, R.A. Livingston, Z. Weldon-Yochim, Rock varnish on architectural stone: microscopy and analysis of nanoscale manganese oxide deposits on the smithsonian castle, Washington, DC, Herit. Sci. 4 (2016) 26, doi:10.1186/s40494-016-0093-2.

[4] Y.M. Mos, A.C. Vermeulen, C.J.N. Buisman, J. Weijma, X-Ray diffraction of iron containing samples: the importance of a suitable configuration, Geomicrobiol. J. 35 (2018) 511–517, doi:10.1080/01490451.2017.1401183.

[5] J. Rathje, M.L. Jackson, Soil Chemical Analysis, Prentice Hall, Inc., Verlag, 1958 Englewood Cliffs, NJ.498 S. DM 39.40, Zeitschrift Für Pflanzenernährung, Düngung, Bodenkunde. 85 (1959) 251–252., doi:10.1002/jpln.19590850311.

[6] R.M. Potter, G.R. Rossman, The manganese- and iron-oxide mineralogy of desert varnish, Chem. Geol. 25 (1979) 79–94, doi:10.1016/0009-2541(79)90085-8.

[7] T. He, J. Li, J. Gray, Y. Gu, Analysis iron distribution methods in fine sand- and silt-sized soil particles, MethodsX 8 (2021) 101248, doi:10.1016/j.mex.2021.101248.

[8] M.E. Brookfield, C.P. Andrews-Speed, Sedimentology, petrography and tectonic significance of the shelf, flysch and molasse clastic deposits across the Indus Suture Zone, Ladakh, NW India, Sediment. Geol. 40 (1984) 249–286, doi:10.1016/0037-0738(84)90011-3.

[9] M.P. Searle, Structural evolution and sequence of thrusting in the High Himalayan, Tibetan-Tethys and Indus suture zones of Zanskar and Ladakh, Western Himalaya, J. Struct. Geol. 8 (1986) 923–936, doi:10.1016/0191-8141(86)90037-4.

[10] E. Garzanti, T. Van Haver, The indus clastics: forearc basin sedimentation in the Ladakh Himalaya (India), Sediment. Geol. 59 (1988) 237–249, doi:10.1016/0037-0738(88)90078-4.

[11] X.H. Xiao, L.Y. Shao, J.Q. Sun, N. Zhang, W.J. Li, Mineral compositions of individual particles in the inhalable particulate matter in the Lanzhou air during heating period, Bull. Miner. Petrol. Geochem. 26 (2007) 64–69.

[12] J. Li, L. Shao, L. Chang, J. Xing, W. Wang, W. Li, D. Zhang, Physicochemical characteristics and possible sources of individual mineral particles in a dust storm episode in Beijing, China, Atmosphere 9 (2018) 269, doi:10.3390/atmos9070269.

[13] S. Jiang, Clay minerals from the perspective of oil and gas exploration, in: M. Valaskova (Ed.), Clay Minerals in Nature-Their Characterization, Modification and Application, InTech, 2012, doi:10.5772/47790.

[14] O.P. Mehra, M.L. Jackson, Iron oxide removal from soils and clays by a dithionite–citrate system buffered with sodium bicarbonate, in: E. Ingerson (Ed.), Clays and Clay Minerals, Pergamon, 2013, pp. 317–327, doi:10.1016/B978-0-08-009235-5.50026-7.

[15] K.R. Kuhlman, W.G. Fusco, M.T. La Duc, L.B. Allenbach, C.L. Ball, G.M. Kuhlman, R.C. Anderson, I.K. Erickson, T. Stuecker, J. Benardini, J.L. Strap, R.L. Crawford, Diversity of microorganisms within rock varnish in the Whipple Mountains, California, Appl. Environ. Microbiol. 72 (2006) 1708–1715, doi:10.1128/AEM.72.2.1708-1715.2006.

[16] C.V. Jeans, D.M. MOORE, R.C. REYNOLDS, X-Ray Diffraction and the Identification and Analysis of Clay Minerals, 2nd Ed, Oxford University Press, Oxford, New York, 1997 xviii + 378 ppPrice £27.95 (spiral-bound paperback). ISBN 0 19 508713 5., Geological Magazine. 135 (1998) 819–842., doi:10.1017/S0016756898501501.

[17] S.T. Smith, R.L. Snyder, W.E. Brownell, Quantitative phase analysis of devonian shales by computer controlled X-Ray diffraction of spray dried samples, Adv. X Ray Anal. 22 (1978) 181–191, doi:10.1154/S0376030800016529.

[18] G.W. Brindley, G. Brown, Crystal structures of clay minerals and their X-Ray identification, (1980). 10.1180/mono-5.

[19] S. Hillier, Quantitative analysis of clay and other minerals in sandstones by X-ray powder diffraction (XRPD), in: R.H. Worden, S. Morad (Eds.), Clay Mineral Cements in Sandstones, Blackwell Publishing Ltd., Oxford, UK, 1999, pp. 213–251, doi:10.1002/9781444304336.ch11.

[20] B. Kubler, M. Jaboyedoff, Illite crystallinity, Compt. Rendus de. Acad. Sci. Paris. 331 (2000) 75–89.

[21] H.J. Kisch, Illite crystallinity: recommendations on sample preparation, X-ray diffraction settings, and interlaboratory samples, J. Metamorph. Geol. 9 (1991) 665–670, doi:10.1111/j.1525-1314.1991.tb00556.x.

[22] C. Spötl, D.W. Houseknecht, R. Jaques, Clay Mineralogy and illite crystallinity of the atoka formation, Arkoma Basin, and frontal ouachita mountains, Clays Clay Miner 41 (1993) 745–754, doi:10.1346/CCMN.1993.0410614.

[23] S. Shata, R. Hesse, R.F. Martin, H. Vali, Expandability of anchizonal illite and chlorite: significance for crystallinity development in the transition from diagenesis to metamorphism, Am. Mineral. 88 (2003) 748–762, doi:10.2138/am-2003-5-604.

[24] H. shirozu, S.W. bailey, Chlorite polytypism: III. Crystal structure of an orthohexagonal iron chlorite, American Mineralogist. 50 (n.d.) 868–885.

[25] V.A. Drits, B.B. Zviagina, D.K. McCarty, A.L. Salyn, Factors responsible for crystal-chemical variations in the solid solutions from illite to aluminoceladonite and from glauconite to celadonite, Am. Mineral. 95 (2010) 348–361, doi:10.2138/am.2010. 3300.

[26] H.M. Rietveld, A profile refinement method for nuclear and magnetic structures, J. Appl. Crystallogr. 2 (1969) 65–71, doi:10. 1107/S0021889869006558.

[27] T. Degen, M. Sadki, E. Bron, U. König, G. Nénert, The highscore suite, Powder Diffr. 29 (2014) S13–S18, doi:10.1017/ S0885715614000840.

[28] Y. PEI, P.Y. CHEN, Table of key lines in x-ray powder diffraction patterns of minerals in clays and associated rocks. (1977).